Construction of a Stable Ru-Re Hybrid System Based on Multifunctional MOF-253 for Efficient Photocatalytic CO₂ Reduction

Xiaoyu Deng, Lizhi Xu, Zhaohui Li[*]

Research Institute of Photocatalysis, State Key Laboratory of Photocatalysis on Energy and Environment, College of Chemistry, Fuzhou University, Fuzhou 350116, People's Republic of China

[*] Author to whom all correspondences should be addressed.
E-mail: zhaohuili1969@yahoo.com (Z. Li), Tel (Fax): 86-591-22865855.

Abstract

Using the open N, N'-chelating sites of MOF-253 (Al(OH)(dcbpy)) (dcbpy=2,2'-bipyridine-5,5'-dicarboxylic acid)to coordinate with Re(I), a surface supported Re complex MOF-253-Re(CO)$_3$Cl active for photocatalytic CO_2 reduction was obtained. Unlike the homogeneous bipyridine containing Re complexes which produced CO during photocatalytic CO_2 reduction, the as-obtained MOF-253-Re(CO)$_3$Cl produced formate as the main CO_2 reduction product. In addition, the surface supported MOF-253-Re(CO)$_3$Cl showed superior photocatalytic performance than its homogeneous counterpart, in which the usual formation of the bimolecular Re intermediate leading to the deactivation of the homogeneous Re complex was significantly inhibited in MOF supported Re complex. To enhance the light absorption of MOF-253-Re(CO)$_3$Cl, a surface supported Ru sensitizer was simultaneously constructed in it. Via an efficient charge transfer from Ru sensitizer to Re catalytic center, which resembles the construction of Ru-Re supramolecular structure using covalent bonds, the Ru sensitizedMOF-253-Re(CO)$_3$Cl showed superior photocatalytic CO_2 reduction under visible light. This study demonstrates the possibility of using MOF with open coordination sites as a multifunctional platform for the construction of stable hybrid systems for artificial photosynthesis.

Introduction

CO$_2$ is a greenhouse gas and the ever increasing combustion of the fossil fuel leads to an excessive emission of CO$_2$ into the atmosphere which results in global warming. [1-5] Although the capture and sequestration of CO$_2$ from post-combustion effluents is an accepted working approach, the use of CO$_2$ as a C1 building block to produce high-value chemicals via catalytic transformations would be more desirable, especially when such a transformation can be realized by utilization of solar light. However, CO$_2$ has exceptional thermodynamic stability and the direct one-electron reduction of CO$_2$ to the radical anion CO$_2{}^{\cdot-}$ is energetically demanding (-1.97 V vs NHE). Although multiple electron reduction products like CO, HCOOH, CH$_3$OH and CH$_4$ can be produced at significantly less negative potentials, their generations are kinetically unfavorable and metal complexes with redox active metal centers and inter-changeable ligands are usually required to realize such multi-electron redox reactions. [6-11] Re^{I} diimine complexes [Re(N, N')(CO)$_3$X] (X=Me, Cl$^-$, etc) have been recognized to be efficient catalysts for CO$_2$ reduction to produce CO or HCOO$^-$ via two-electron proton coupled reduction pathways. [12-18] However, these Re diimine complexes showed poor absorption in visible light region. To be applied in photocatalytic CO$_2$ reduction under visible light, bimetallic M-Re (M=Ru, Ir, Os) supramolecular structures by attaching Re complexes to photosensitizers via covalent bonds should be constructed. [19-24] However, the preparations of such supramolecules are usually challenging and tedious. In addition, these supramolecules also suffer from all the disadvantages of being homogeneous catalysts, like the difficultly in separation from the reaction systems for recycling.

The use of porous materials as supports to heterogenize the homogeneous catalysts is a generally adopted strategy. [25-29] Metal-organic frameworks (MOFs), a class of porous materials constructed from the metal/metal clusters and poly-dentated organic ligands, have been targeted as attractive supports for the molecular catalysts over the past years, due to their well-defined and highly tunable porous structures. [29-45] MOFs can offer or be endowed with well defined isolated sites for anchoring of catalytic active species. Actually, MOFs-supported molecular catalysts for a variety of organic transformations have been obtained. [46-49] Especially, a direct construction of metal complexes using MOFs themselves as solid ligand is an ideal

strategy to develop supported molecular catalysts without losing their performance. [25, 50, 51] With opening N, N'-chelating sites in its structure, MOF-253 (Al(OH)(dcbpy)) (dcbpy=2,2'-bipyridine-5,5'-dicarboxylic acid) is an ideal solid ligand for construction of surface supported metal complex featuring bpy ligands. Actually several previous studies have already been conducted on the functionalizations of MOF-253 with Ru, Pt, Ln (Ln = Eu, Tb, Sm) containing complexes using its open N, N'-chelating sites. [52-55]

Herein, we reported the use of open N, N'-chelating sites in MOF-253 to construct supported active Re carbonyl complex MOF-253-Re(CO)$_3$Cl for photocatalytic CO_2 reduction under visible light. Unlike the homogeneous bipyridine containing Re complexes which produced CO during photocatalytic CO_2 reduction, the as-obtained MOF-253-Re(CO)$_3$Cl produced formate as the main CO_2 reduction product. The as-obtained MOF-253-Re(CO)$_3$Cl is more stable than its homogeneous counterpart Re(dcbpy)(CO)$_3$Cl since the usual formation of the bimolecular Re intermediate leading to the deactivation of the homogeneous Re complex was significantly inhibited in MOF supported Re complex ascribed to the spatially isolated Re moieties in MOF-253. [56-57] To enhance the light absorption capability of MOF-253-Re(CO)$_3$Cl, a surface supported Ru sensitizer was simultaneously constructed in MOF-253-Re(CO)$_3$Cl. Via an efficient charge transfer from Ru sensitizer to Re catalytic center, the Ru sensitized-MOF-253-Re(CO)$_3$Cl show superior performance for photocatalytic CO_2 reduction under visible light. The use of MOF-253 as a platform for assembling Ru photosensitizer and Re catalyst resembles the construction of the light chromophores with catalytic components via covalent bonds to form the supramolecular structures reported previously, but is more facile in synthesis. This study demonstrates the possibility of using MOF with open coordination sites as a multifunctional platform for the construction of stable hybrid systems for artificial photosynthesis.

Experimental

Preparations

All the chemicals were obtained commercially and used without further purifications. MOF-253 was synthesized following the previous literature. [52] MOF-253-Re(CO)$_3$Cl was synthesized from MOF-253 and Re(CO)$_5$Cl under refluxing. Before reaction, MOF-253 was de-solvated under vacuum at 150 °C overnight. The vacuum-treated MOF-253 (428.7 mg, 1.5 mmol) and Re(CO)$_5$Cl

(108.5 mg, 0.3 mmol) were refluxed in anhydrous toluene (60 ml) for 2 h in N_2 atmosphere. After the reaction, the resultant powder was filtered, washed with MeOH and dried under vacuum to give the yellow product (147.2 mg, 83%).

Sensitized-MOF-253-Re(CO)$_3$Cl was prepared by reacting MOF-253-Re(CO)$_3$Cl with Ru(bpy)$_2$Cl$_2$ (bpy=2,2'-bipyridine) in MeOH. Ru(bpy)$_2$Cl$_2$ (2.0 mg, 2.6 μmol) was dissolved in a minimum amount of MeOH. MOF-253-Re(CO)$_3$Cl (50.0 mg) was added to the above solution and the resultant suspension was incubated at room temperature for 12 h. The resultant product was washed with MeOH for several times and dried at 60 ℃ under vacuum to obtain a deep orange powder. For comparison, Ru(bpy)$_2$Cl$_2$ supported on MOF-253 (MOF-253-Ru) was prepared by reacting Ru(bpy)$_2$Cl$_2$ with MOF-253.

Homogeneous Re(dcbpy)(CO)$_3$Cl was prepared according to the method reported previously with slight modifications. [18, 58] Re(CO)$_5$C1 (289 mg, 0.8mmol) was dissolved in toluene at 60 °C and dcbpy (195 mg, 0.8 mmol) was added to the above solution, causing a color change from pale yellow to deep red. The mixture was stirred and heated at 80 °C for 2 h. The suspension was filtered and the product was washed with MeOH and dried under vacuum to obtain the red product.

Characterizations

X-ray diffraction (XRD) patterns were collected on a Bruker D8 Advance X-ray diffractometer with Cu K$_\alpha$ radiation. The accelerating voltage and the applied current were 40 KV and 40 mA, respectively. Data were recorded at a scan rate of 0.05° 2θ s^{-1} in the 2θ range from 5° to 40°. The IR spectra were obtained on a Nicolet 670 FT-IR spectrometer. UV-vis diffuse-reflectance spectrometry (UV-vis DRS) were obtained on a UV-visible spectrophotometer (Cary 500 Scan Spectrophotometers, Varian). BaSO$_4$ was used as a reference. N_2 adsorption/desorption isotherms was carried out at 77 K on ASAP2020 apparatus (Micromeritics Instrument Corp., USA). Inductively Coupled Optical Emission Spectrometry (ICP-OES) was performed on an Optima 8000 (PerkinElmer). The sample was digested in a mixture of HNO$_3$ and Milli-Q water. EI-MS were detected with Agilent 5977A spectrometer. NMR spectra were obtained on a 400MHz broker AVANCE Ⅲ 400 system (400 MHz).

Photocatalytic CO$_2$ reduction

Photocatalyst (5 mg) was vacuumed and purged with CO_2. A mixture of DMF, TEOA and H$_2$O (4ml) in a volume ratio of 5:1:0.2, degassed and saturated with CO_2

to remove any dissolved O_2, was injected into the reaction tube. The reaction was carried out under the irradiation of Xe lamp with a UV-cut filter to remove all irradiations with wavelength lower than 420 nm and an IR-cut filter to remove those with wavelength longer than 800 nm. After the reaction, the amount of produced $HCOO^-$ was determined by ion chromatography (881 Compact IC pro, Metrosep) with Metrosep A supp 5 250/4.0 column. A mixture of 3.2 mM Na_2CO_3 and 1.0 mM $NaHCO_3$ was used as the eluent. The gaseous products were analyzed by GC-TCD (Shimadzu GC-2014) with a TDX-01 packed column. ^{13}CO performed by Agilent 7890B-5977A GC-MS.

Results and discussion

MOF-253 with high quality was synthesized following the previously reported method. To prepare MOF-253-Re(CO)$_3$Cl, the as-synthesized MOF-253 was de-solvated under dynamic vacuum and then refluxed in anhydrous toluene solution containing Re(CO)$_5$Cl. During the reaction, the color of the suspension changed from pale yellow to orange, indicating the reaction between the MOF-253 and Re complex did occur. The XRD pattern of the as-synthesized product shows characteristic diffraction peaks of the MOF-253 framework, indicating that the introduction of the Re moiety does not influence the structure of MOF-253 (Fig. 1a). The slight decrease of the diffraction intensity of the resultant product as compared with the parent MOF-253 is probably due to the existence of disorder within the crystal structure of MOF-253 after the immobilization of the Re complex. The presence of Re species in the as-prepared product was confirmed by its FT-IR spectrum (Fig. 1b). As compared with the parent MOF-253, four additional peaks at 2027 cm^{-1}, 2024 cm^{-1}, 1920 cm^{-1} and 1903 cm^{-1} assignable to the asymmetric vibration of CO are observed, indicative of the formation of MOF-253-Re(CO)$_3$Cl. The coordination of Re^{I} to free N, N'-chelating sites in MOF-253 leads to a slight red shift of the asymmetric vibration of CO as compared with those in the original Re(CO)$_5$Cl, which locates in 2060 cm^{-1}, 2036 cm^{-1} and 1971 cm^{-1}, 1959 cm^{-1}. The introduction of Re species into MOF-253 leads to a slightly decrease of the Langmuir surface area from the original 1489 cm^3/g for pristine MOF-253 to 973 cm^3/g for MOF-253-Re(CO)$_3$Cl, which can be attributed to the partial blocking of the pores in MOF-253 by the Re carbonyl complex. The relatively high Langmuir specific surface area of MOF-253-Re(CO)$_3$Cl still indicates the existence of the permanent porosity and the framework of MOF-253 is retained

(Fig. 1c). ICP of the digested MOF sample gave a Re/Al molar ratio of 14.9% in the as-obtained MOF-253-Re(CO)$_3$Cl, which is a little lower than that added into the reaction system (with Re/Al at 20%). All these suggested that MOF-253-Re(CO)$_3$Cl had successfully been obtained

The UV-vis DRS spectrum of the as-obtained MOF-253-Re(CO)$_3$Cl, together with that of pure MOF-253 and Re(dcbpy)(CO)$_3$Cl, are shown in Fig. 1d. In accordance with its yellow color in solution, homogeneous Re(dcbpy)(CO)$_3$Cl shows an absorption centering at 390 nm and extends to 476 nm, which can be assigned to the metal-to-ligand (Re^I to π* of bipyridine) charge transfer (MLCT). Pure MOF-253 alone does not show absorption in the visible light region. However, when MOF-253 was coordinated to Re(I) via the open N, N'-chelating sites, the as-prepared MOF-253-Re(CO)$_3$Cl shows absorption centering at 395 nm and extends to 540 nm. As compared with homogeneous Re(dcbpy)(CO)$_3$Cl, a red shift was observed, indicative of the existence of strong interaction between [Re(CO)$_3$Cl] moiety and MOF-253 framework.

Considering that diimine containing Re carbonyl complexes are good catalysts for CO$_2$ reduction, the performance for photocatalytic CO$_2$ reduction over the as-obtained MOF-253-Re(CO)$_3$Cl was investigated. [58-60] The reaction was initially carried out in a CO$_2$ saturated mixed solvent of DMF/H$_2$O (25/1) in the presence of triethanolamine (TEOA) as the sacrificial agent under visible light. Photocatalytic CO$_2$ reduction over the as-prepared MOF-253-Re(CO)$_3$Cl produced HCOO$^-$, CO and little H$_2$, the amount of all the products increased with the irradiation time(Fig. 2a). After 4h about 9.50 μmol of HCOO$^-$, 2.23 μmol of CO as well as 0.11 μmol of H$_2$

were produced, corresponding to TON for the formation of HCOO$^-$, CO and H$_2$ to be 10.0, 2.4 and 0.1, respectively (Table 1, entry 1). No products were detected over pure MOF-253 or MOF-253-Re(CO)$_3$Cl without light irradiation (Table 1, entry 2 and 3), indicating that the formation of the products was induced by photocatalysis over MOF-253-Re(CO)$_3$Cl. Only 0.22 μmol of H$_2$ (TON = 0.23) was produced under the N$_2$ atmosphere, implying that CO and HCOO$^-$ came from the reduction of CO$_2$ (Table 1, entry 4). The reaction medium as well as the sacrificial agent influenced the photocatalytic activity. The change of the solvent from DMF to THF led to a decrease

of the t-TON (t-TON for total TON of the produced CO and HCOO$^-$) from 12.37 to 5.77 (Table 1, entry 5). Sacrificial agent play an important role in the photoctalytic CO_2 reduction since a much lower t-TON (1.58) was obtained when the sacrificial agent TEOA was replaced by TEA and no products were detected in absence of the sacrificial agent (Table 1, entry 6, 7). Although CO_2 can be photocatalytic reduced over homogeneous Re(dcbpy)(CO)$_3$Cl, the main product obtained was CO and in 4h, a t-TON of 9.37 were obtained (Table 1, entry 8).

As compared with the homogeneous Re(dcbpy)(CO)$_3$Cl, MOF-253-Re(CO)$_3$Cl showed higher stability during the photocatalytic CO_2 reduction. The amount of all the products increased with the irradiation time and a t-TON of 24.35 for photocatalytic CO_2 reduction was obtained in 16 h (Fig. 2b). Although the ICP analysis revealed that about 1.6 % of the incorporated Re leached into the reaction filtrate, the filtrate experiment showed no more HCOO$^-$ were produced and none CO was detected when the filtrate was irradiated for another 4 h (Fig. 2a), a confirmation of the heterogeneous nature of the MOF-253-Re(CO)$_3$Cl in the photocatalytic CO_2 reduction. Moreover, the XRD of the MOF-253-Re(CO)$_3$Cl did not change obviously after the reaction (Fig 3). All these observations indicated that MOF-253-Re(CO)$_3$Cl is stable during photocatalytic CO_2 reduction. However, the color of the homogeneous Re(dcbpy)(CO)$_3$Cl reaction system changed gradually from the original yellow to colorless during the reaction and the amount of the produced CO did not increase after 4 h irradiations, indicating the deactivation of the homogeneous Re complex (Fig 2b).

Previous studies indicated that the deactivation of the homogeneous Re(N, N')(CO)$_3$Cl during CO_2 reduction is induced by the formation of the inactive bimolecular [Re(N, N')(CO)$_3$]$_2$OCO$_2$. [57, 61] It is generally believed that when homogeneous Re(N, N')(CO)$_3$Cl is excited, the dissociation of Cl$^-$ gives penta-coordinated [Re(N, N')(CO)$_3$] as the intermediate, which can reduce CO_2 to give CO via two pathways. [47, 62, 63] The predominant pathway involves a very fast CO_2 addition to generate a CO_2 bridged [Re(N, N')(CO)$_3$]$_2$C(O)O, which followed by the addition of another CO_2 and the release of CO to give the inactive [Re(N, N'(CO)$_3$]$_2$OCO$_2$ and terminate the reaction. Another slow pathway, ie, non-dominant one, is the addition of CO_2 to [Re(N, N')(CO)$_3$] to generate Re(N, N')(CO)$_3$COOH, which can also release CO and return back to [Re(N, N')(CO)$_3$Cl]. Since the

predominant pathway during the CO_2 reduction over homogeneous $Re(N, N')(CO)_3Cl$ give the nonactive bimolecular $[Re(N, N')(CO)_3]_2C(O)O$, homogeneous Re complexes deactivate very fast during the photocatalytic CO_2 reduction (Scheme 1)

On the contrary, although light irradiation on $MOF-253-Re(CO)_3Cl$ also lead to the one-electron reduced species $[MOF-253-Re(CO)_3]$ by releasing a Cl^-, two spatially isolated $[(N,N')-Re(CO)_3]$ in MOF-253 cannot be bridged by CO_2 to generate the non-active bimolecular $[MOF-253-Re(CO)_3]_2C(O)O$. Therefore, the deactivation of the active Re species by forming the inactive bimolecular $[MOF-253-Re(CO)_3]_2OCO_2$ can be significantly inhibited in the surface supported Re complexes. However, the direct CO_2 adduction into the Re-hydride $[MOF-253-Re(CO)_3H]$ is possible to form $[MOF-253-Re(CO)_3OCHO]$, which leads to the production of $HCOO^-$ and recover the $[MOF-253-Re(CO)_3Cl]$. [64] Although no production of $HCOO^-$ was isolated during the photocatalytic CO_2 reduction over homogeneous $Re(N, N')(CO)_3Cl$, the study by Hawecker et. al. directly observed the formate-intermediate $Re(N, N')(CO)_3OCHO$. [17] In addition, Re hydride intermediate $Re(N, N')(CO)_3H$ has previously been used for CO_2 reduction to produce $HCOO^-$. [65] A non-dominant pathway also exists to produce CO via the addition of CO_2 to $[MOF-253-Re(CO)_3]$ for generating $MOF-253-Re(CO)_3COOH$, which is similar to that observed in homogeneous $Re(N, N')(CO)_3Cl$ system. Since the direct addition of CO_2 to $[MOF-253-Re(CO)_3]$ is slow, the main product from CO_2 reduction over $MOF-253-Re(CO)_3Cl$ is $HCOO^-$ (Scheme 2).

The above mechanism for photocatalytic CO_2 reduction was verified by the reaction carried out using $^{13}CO_2$. The GC-MS spectra of the gaseous product from the reaction with $^{13}CO_2$ show signals at m/z values of 29 and 28, corresponding to ^{13}CO and ^{12}CO respectively. In contrast, only the signal at the m/z value of 28 was detected in the product from the reaction with $^{12}CO_2$. This clearly indicates that CO_2 was reduced to CO over $MOF-253-Re(CO)_3Cl$ (Supporting Fig. 1). The coexistence of ^{12}CO in the gaseous product in the $^{13}CO_2$ reaction may come from those dissociated from the $MOF-253-Re(CO)_3Cl$ as elucidated in the mechanism. Also the $HCOO^-$ is originated from CO_2 as evidenced from the ^{13}C NMR spectrum (Supporting Fig. 2).

The disadvantage of using $[Re(N, N')(CO)_3X]$ complexes for photocatalytic CO_2

reduction is their poor light absorption in the visible light region. The coupling of a Ru photosensitizer to the Re catalyst via building Ru(II)–Re(I) supramolecules have been demonstrated to be an effective method to improve their photocatalytic performance for CO_2 reduction under visible light. [66-68] However, the syntheses of the supramolecules are usually challenging and require tedious process. MOFs provides an appealing platform for assembly of different active components into an efficient composite photocatalytic system due to its highly ordered crystalline structure, which can promote the charge transfer between the photosensitizer and the surface constructed catalyst. [69-72] That is to say the tailorable character of MOFs allows a huge flexibility to assemble multi-functional material for applications. [41, 73-76] Therefore, to further improve the light absorption of MOF-253-Re(CO)$_3$Cl, Ru(bpy)$_2$Cl$_2$ was used to prepared photo-sensitized MOF-253-Re(CO)$_3$Cl since Ru(bpy)$_2$Cl$_2$ can also react with the surface N, N'-chelate sites to form MOF-253 supported [Ru(N, N')(bpy)$_2^{2+}$], which shows absorption in visible light region. [55] As shown in Fig 1d, sensitized-MOF-253-Re(CO)$_3$Cl shows enhanced absorption in visible light region, with the absorption edge extending to 648 nm. The formation of [Ru(N, N')(bpy)$_2^{2+}$] was also confirmed by the higher catalytic activity over MOF-253 supported Ru(bpy)$_2$Cl$_2$ (MOF-253-Ru) (TON of HCOO$^-$ and CO to be 0.6

and 0.08, respectively) than that over pure Ru(bpy)$_2$Cl$_2$ with TON of HCOO$^-$ and CO to be 0.1 and 0.02) under similar conditions (Table 1, entry 10 and 11). The photocatalytic activity over the sensitized-MOF-253-Re(CO)$_3$Cl was found to increase significantly as compared with the non-sensitized one. The TON of HCOO$^-$, CO and H$_2$ produced in 4 h over sensitized MOF-253-Re(CO)$_3$Cl, with a molar ratio of Ru(bpy)$_2$Cl$_2$/Re-complex at 1 : 32, was determined to be 23.26, 5.40 and 0.99, nearly twice higher than MOF-253-Re(CO)$_3$Cl under similar conditions (Fig 4). ICP analyses showed that about 1.4% of Ru leached into the solution after 4 h of irradiation. However, the amount of Ru leaching into solution did not influence the photocatalytic activity since homogeneous Ru(bpy)$_2$Cl$_2$ exhibited low activity under similar conditions (Table 1, entry 11). These indicates that the photocatalytic CO_2 reduction did occur over heterogeneous sensitized-MOF-253-Re(CO)$_3$Cl. It is means that MOF-253 can act as a multifunction plantform to supported photocatalyst Re complex and photosensitizer Ru complex to construct a stable hybrid photocatalysis

system, which can promote the charge transfer between the photosensitizer and the photocatalyst.

Conclusions

In summary, MOF-253 surface constructed Re carbonyl complex MOF-253-Re(CO)$_3$Cl shows superior photocatalytic performance for CO_2 reduction under visible light irradiation as compared with its homogeneouscounterpart. In addition, a surface supported Ru sensitizer was simultaneously constructed in MOF-253-Re(CO)$_3$Cl to give a sensitized-MOF-253-Re(CO)$_3$Cl, which shows a superior performance for photocatalytic CO_2 reduction under visible light via an efficient charge transfer from Ru sensitizer to Re catalytic center. This work highlights the great potential of using MOFs both as a solid ligand to build a supported molecular catalyst and as a platform for assembly of several active moieties into one composite system to achieve complicated functions.

Reference

[1]   Song C 2006 Global challenges and strategies for control, conversion and utilization of CO_2 for sustainable development involving energy, catalysis, adsorption and chemical processing *Catal. Today* **115** 2-32

[2]   Lewis N S and Nocera D G 2006 Powering the planet: Chemical challenges in solar energy utilization *Proc. Nat.l Acad. Sci.* **103** 15729-35

[3]   Fontecave M 2011 Energy for a Sustainable World. From the Oil Age to a Sun-Powered Future. By Nicola Armaroli and Vincenzo Balzani *Angew. Chem. Int. Edit.* **50** 6704-5

[4]   Appel A M, Bercaw J E, Bocarsly A B, Dobbek H, DuBois D L, Dupuis M, Ferry J G, Fujita E, Hille R, Kenis P J, Kerfeld C A, Morris R H, Peden C H, Portis A R, Ragsdale S W, Rauchfuss T B, Reek J N, Seefeldt L C, Thauer R K and Waldrop G L 2013 Frontiers, opportunities, and challenges in biochemical and chemical catalysis of CO_2 fixation *Chem. Rev.* **113** 6621-58

[5]   Habisreutinger S N, Schmidt-Mende L and Stolarczyk J K 2013 Photocatalytic reduction of CO_2 on TiO_2 and other semiconductors *Angew. Chem. Int. Edit.* **52** 7372-408

[6]   Chang X, Wang T and Gong J 2016 CO_2 photo-reduction: insights into CO_2 activation and reaction on surfaces of photocatalysts *Energy Environ. Sci.* **9** 2177-96

[7]   Liu X, Inagaki S and Gong J 2016 Heterogeneous Molecular Systems for Photocatalytic CO_2 Reduction with Water Oxidation *Angew. Chem. Int. Edit.* **55** 14924-50

[8]   White J L, Baruch M F, Pander Iii J E, Hu Y, Fortmeyer I C, Park J E, Zhang T, Liao K, Gu J, Yan Y, Shaw T W, Abelev E and Bocarsly A B 2015 Light-Driven Heterogeneous Reduction of Carbon Dioxide: Photocatalysts and Photoelectrodes *Chem. Rev.* **115** 12888-935

[9]   Ashford D L, Gish M K, Vannucci A K, Brennaman M K, Templeton J L, Papanikolas J M and Meyer T J 2015 Molecular Chromophore-Catalyst Assemblies for Solar Fuel Applications *Chem. Rev.* **115** 13006-49

[10]   Tu W, Zhou Y and Zou Z 2014 Photocatalytic conversion of CO_2 into renewable hydrocarbon fuels: state-of-the-art accomplishment, challenges, and prospects *Adv. Mater.* **26** 4607-26

[11]   Marszewski M, Cao S, Yu J and Jaroniec M 2015 Semiconductor-based photocatalytic CO_2 conversion *Mater. Horiz.* **2** 261-78

[12]   Kotch T G, Lees A J, Fuerniss S J and Papathomas K I 1992 Luminescent organometallic complexes as visible probes in the isothermal curing of epoxy resins *Chem. Mater.* **4** 675-83

[13]   Kumar B, Smieja J M and Kubiak C P 2010 Photoreduction of CO_2 on p-type Silicon Using Re (bipy-Bu-*t*)$(CO)_3$Cl: Photovoltages Exceeding 600 mV for the Selective Reduction of CO_2 to CO *J. Phys. Chem. C* **114** 14220-3

[14]   Smieja J M and Kubiak C P 2010 Re(bipy-tBu)$(CO)_3$Cl-improved catalytic activity for

reduction of carbon dioxide: IR-spectroelectrochemical and mechanistic studies *Inorg. Chem.* **49** 9283-9

[15] Kumar B, Llorente M, Froehlich J, Dang T, Sathrum A and Kubiak C P 2012 Photochemical and photoelectrochemical reduction of CO_2 *Annu. Rev. Phys. Chem.* **63** 541-69

[16] Portenkirchner E, Apaydin D, Aufischer G, Havlicek M, White M, Scharber M C and Sariciftci N S 2014 Photoinduced energy transfer from poly(N-vinylcarbazole) to tricarbonylchloro-(2,2'-bipyridyl)rhenium(I) *Chemphyschem* **15** 3634-8

[17] Hawecker J, Lehn J M and Ziessel R 1986 Photochemical and Electrochemical Reduction of Carbon Dioxide to Carbon Monoxide Mediated by (2, 2′-Bipyridine) tricarbonylchlororhenium (I) and Related Complexes as Homogeneous Catalysts *Helv. Chim. Acta* **69** 1990-2012

[18] Juris A, Campagna S, Bidd I, Lehn J M and Ziessel R 1988 Synthesis and photophysical and electrochemical properties of new halotricarbonyl(polypyridine)rhenium(I) complexes *Inorg. Chem.* **27** 4007-11

[19] Ali N M, MacLeod V L, Jennison P, Sazanovich I V, Hunter C A, Weinstein J A and Ward M D 2012 Luminescent cyanometallates based on phenylpyridine-Ir(III) units: solvatochromism, metallochromism, and energy-transfer in Ir/Ln and Ir/Re complexes *Dalton Trans.* **41** 2408-19

[20] Ohkubo K, Yamazaki Y, Nakashima T, Tamaki Y, Koike K and Ishitani O 2016 Photocatalyses of Ru(II)–Re(I) binuclear complexes connected through two ethylene chains for CO_2 reduction *J. Cata.* **343** 278-89

[21] Sahara G, Kumagai H, Maeda K, Kaeffer N, Artero V, Higashi M, Abe R and Ishitani O 2016 Photoelectrochemical Reduction of CO_2 Coupled to Water Oxidation Using a Photocathode With a Ru(II)-Re(I) Complex Photocatalyst and a CoOx/TaON Photoanode *J. Am. Chem. Soc.*

[22] Fan Y, Zhang L Y, Dai F R, Shi L X and Chen Z N 2008 Preparation, Characterization, and Photophysical Properties of Pt−M (M = Ru, Re) Heteronuclear Complexes with 1,10-Phenanthrolineethynyl Ligands *Inorg. Chem.* **47** 2811-9

[23] Shankar B, Arumugam R, Elumalai P and Sathiyendiran M 2016 Rhenium(I)-Based Monocyclic and Bicyclic Phosphine Oxide-Coordinated Supramolecular Complexes *ACS Omega* **1** 507-17

[24] Cavigli P, Balducci G, Zangrando E, Demitri N, Amati A, Indelli M T and Iengo E 2016 Structural and photophysical characterization of a tin(IV) porphyrin–rhenium(I)(diimine) conjugate *Inorg. Chim. Acta* **439** 61-8

[25] Wang C, Xie Z, deKrafft K E and Lin W 2011 Doping metal-organic frameworks for water oxidation, carbon dioxide reduction, and organic photocatalysis *J. Am. Chem. Soc.* **133** 13445-54

[26]   Windle C D, Pastor E, Reynal A, Whitwood A C, Vaynzof Y, Durrant J R, Perutz R N and Reisner E 2015 Improving the photocatalytic reduction of CO2 to CO through immobilisation of a molecular Re catalyst on TiO2 *Chem. Eur. J.* **21** 3746-54

[27]   Wang X, Shi H, Kwak J H and Szanyi J 2015 Mechanism of CO_2 Hydrogenation on Pd/Al_2O_3 Catalysts: Kinetics and Transient DRIFTS-MS Studies *ACS Catal.* **5** 6337-49

[28]   Wu F, Feng Y and Jones C W 2014 Recyclable Silica-Supported Iridium Bipyridine Catalyst for Aromatic C–H Borylation *ACS Catal.* **4** 1365-75

[29]   Corma A, Garcia H and Xamena F X L I 2010 Engineering Metal Organic Frameworks for Heterogeneous Catalysis *Chem. Rev.* **110** 4606-55

[30]   Van de Voorde B, Bueken B, Denayer J and De Vos D 2014 Adsorptive separation on metal-organic frameworks in the liquid phase *Chem. Soc. Rev.* **43** 5766-88

[31]   Furukawa H, Cordova K E, O'Keeffe M and Yaghi O M 2013 The chemistry and applications of metal-organic frameworks *Science* **341** 1230444

[32]   Suh M P, Park H J, Prasad T K and Lim D W 2012 Hydrogen storage in metal-organic frameworks *Chem. Rev.* **112** 782-835

[33]   Zhou H C, Long J R and Yaghi O M 2012 Introduction to metal-organic frameworks *Chem. Rev.* **112** 673-4

[34]   Xuan W, Zhu C, Liu Y and Cui Y 2012 Mesoporous metal-organic framework materials *Chem. Soc. Rev.* **41** 1677-95

[35]   Gao W Y, Chrzanowski M and Ma S 2014 Metal-metalloporphyrin frameworks: a resurging class of functional materials *Chem. Soc. Rev.* **43** 5841-66

[36]   Lee J, Farha O K, Roberts J, Scheidt K A, Nguyen S T and Hupp J T 2009 Metal-organic framework materials as catalysts *Chem. Soc. Rev.* **38** 1450-9

[37]   Kreno L E, Leong K, Farha O K, Allendorf M, Van Duyne R P and Hupp J T 2012 Metal-organic framework materials as chemical sensors *Chem. Rev.* **112** 1105-25

[38]   Zhou H C and Kitagawa S 2014 Metal-organic frameworks (MOFs) *Chem. Soc. Rev.* **43** 5415-8

[39]   Li J R, Sculley J and Zhou H C 2012 Metal-organic frameworks for separations *Chem. Rev.* **112** 869-932

[40]   Horcajada P, Gref R, Baati T, Allan P K, Maurin G, Couvreur P, Ferey G, Morris R E and Serre C 2012 Metal-organic frameworks in biomedicine *Chem. Rev.* **112** 1232-68

[41]   Huang Y B, Liang J, Wang X S and Cao R 2017 Multifunctional metal-organic framework catalysts: synergistic catalysis and tandem reactions *Chem. Soc. Rev.* **46** 126-57

[42]   Jiang H L and Xu Q 2011 Porous metal-organic frameworks as platforms for functional applications *Chem. Commun.* **47** 3351-70

[43]   Stock N and Biswas S 2012 Synthesis of metal-organic frameworks (MOFs): routes to various MOF topologies, morphologies, and composites *Chem. Rev.* **112** 933-69

[44]   Lu W, Wei Z, Gu Z Y, Liu T F, Park J, Park J, Tian J, Zhang M, Zhang Q and Rd G T 2014 Tuning the structure and function of metal-organic frameworks via linker design *Chem. Soc. Rev.* **43** 5561-93

[45]   He Y, Li B, O'Keeffe M and Chen B 2014 Multifunctional metal-organic frameworks constructed from meta-benzenedicarboxylate units *Chem. Soc. Rev.* **43** 5618-56

[46]   Bai C, Yao X and Li Y 2015 Easy Access to Amides through Aldehydic C–H Bond Functionalization Catalyzed by Heterogeneous Co-Based Catalysts *ACS Catal.* **5** 884-91

[47]   Fei H and Cohen S M 2015 Metalation of a thiocatechol-functionalized Zr(IV)-based metal-organic framework for selective C-H functionalization *J. Am. Chem. Soc.* **137** 2191-4

[48]   Cho S H, Ma B, Nguyen S T, Hupp J T and Albrecht-Schmitt T E 2006 A metal-organic framework material that functions as an enantioselective catalyst for olefin epoxidation *Chem. Commun.* 2563-5

[49]   Horike S, Dinca M, Tamaki K and Long J R 2008 Size-selective Lewis acid catalysis in a microporous metal-organic framework with exposed Mn2+ coordination sites *J. Am. Chem. Soc.* **130** 5854-5

[50]   Li L, Zhang S, Xu L, Han L, Chen Z N and Luo J 2013 An intensely luminescent metal-organic framework based on a highly light-harvesting dyclo-metalated iridium(III) unit showing effective detection of explosives *Inorg. Chem.* **52** 12323-5

[51]   Fei H, Sampson M D, Lee Y, Kubiak C P and Cohen S M 2015 Photocatalytic CO_2 Reduction to Formate Using a Mn(I) Molecular Catalyst in a Robust Metal-Organic Framework *Inorg. Chem.* **54** 6821-8

[52]   Bloch E D, Britt D, Lee C, Doonan C J, Uribe-Romo F J, Furukawa H, Long J R and Yaghi O M 2010 Metal insertion in a microporous metal− organic framework lined with 2, 2′-bipyridine *J. Am. Chem. Soc.* **132** 14382-4

[53]   Zhou T, Du Y, Borgna A, Hong J, Wang Y, Han J, Zhang W and Xu R 2013 Post-synthesis modification of a metal–organic framework to construct a bifunctional photocatalyst for hydrogen production *Energy Environ. Sci.* **6** 3229

[54]   Lu Y and Yan B 2014 Luminescent lanthanide barcodes based on postsynthetic modified nanoscale metal–organic frameworks *J. Mater. Chem. C* **2** 7411

[55]   Sun D, Gao Y, Fu J, Zeng X, Chen Z and Li Z 2015 Construction of a supported Ru complex on bifunctional MOF-253 for photocatalytic CO2 reduction under visible light *Chem. Commun.* **51** 2645-8

[56]   Gibson D H, Yin X, He H and Mashuta M S 2003 Synthesis and Reactions of fac-[Re (dmbpy)(CO) 3X](dmbpy= 4, 4'-Dimethyl-2, 2'-bipyridine; X= COOH, CHO) and Their Derivatives *Organometallics* **22** 337-46

[57]   Agarwal J, Fujita E, Schaefer H F, 3rd and Muckerman J T 2012 Mechanisms for CO production from CO_2 using reduced rhenium tricarbonyl catalysts *J. Am. Chem. Soc.* **134**

5180-6

[58] Manbeck G F, Muckerman J T, Szalda D J, Himeda Y and Fujita E 2015 Push or Pull? Proton Responsive Ligand Effects in Rhenium Tricarbonyl CO_2 Reduction Catalysts *J. Phys. Chem. B* **119** 7457-66

[59] Bruckmeier C, Lehenmeier M W, Reithmeier R, Rieger B, Herranz J and Kavakli C 2012 Binuclear rhenium(I) complexes for the photocatalytic reduction of CO_2 *Dalton Trans.* **41** 5026-37

[60] Agarwal J, Sanders B C, Fujita E, Schaefer H F, 3rd, Harrop T C and Muckerman J T 2012 Exploring the intermediates of photochemical CO_2 reduction: reaction of $Re(dmb)(CO)_3COOH$ with CO_2 *Chem. Commun.* **48** 6797-9

[61] Takeda H, Koike K, Inoue H and Ishitani O 2008 Development of an efficient photocatalytic system for CO_2 reduction using rhenium (I) complexes based on mechanistic studies *J. Am. Chem. Soc.* **130** 2023-31

[62] Gibson D H and Yin X 1998 Synthesis and Reactions of fac-Re $(dmbpy)(CO)_3X$ (dmbpy= 4, 4'-dimethyl-2, 2'-bipyridyl; X= COOH, COOMe, H, OH, and OCHO) *J. Am. Chem. Soc.* **120** 11200-1

[63] Schneider T W, Ertem M Z, Muckerman J T and Angeles-Boza A M 2016 Mechanism of Photocatalytic Reduction of CO_2 by $Re(bpy)(CO)_3Cl$ from Differences in Carbon Isotope Discrimination *ACS Catal.* **6** 5473-81

[64] Grills D C and Fujita E 2010 New Directions for the Photocatalytic Reduction of CO_2: Supramolecular, $scCO_2$ or Biphasic Ionic Liquid−$scCO_2$ Systems *J. Phys. Chem. Lett.* **1** 2709-18

[65] Sullivan B P and Meyer T J 1986 Kinetics and mechanism of carbon dioxide insertion into a metal-hydride bond. A large solvent effect and an inverse kinetic isotope effect *Organometallics* **5** 1500-2

[66] Yamamoto Y, Tamaki Y, Yui T, Koike K and Ishitani O 2010 New Light-Harvesting Molecular Systems Constructed with a Ru (II) Complex and a Linear-Shaped Re (I) Oligomer *J. Am. Chem. Soc.* **132** 11743-52

[67] Nakada A, Koike K, Nakashima T, Morimoto T and Ishitani O 2015 Photocatalytic CO_2 reduction to formic acid using a Ru(II)-Re(I) supramolecular complex in an aqueous solution *Inorg. Chem.* **54** 1800-7

[68] Nakada A, Koike K, Maeda K and Ishitani O 2016 Highly efficient visible-light-driven CO_2 reduction to CO using a Ru(ii)–Re(i) supramolecular photocatalyst in an aqueous solution *Green Chem.* **18** 139-43

[69] Crake A, Christoforidis K C, Kafizas A, Zafeiratos S and Petit C 2017 CO_2 capture and photocatalytic reduction using bifunctional TiO_2 /MOF nanocomposites under UV–vis irradiation *Appl. Cata. B-Environ* **210** 131-40

[70] Wang J L, Wang C and Lin W 2017 Metal–Organic Frameworks for Light Harvesting and

Photocatalysis *Acs Catal.* **2** 2630–40

[71]   Sun D and Li Z 2017 Robust Ti- and Zr-Based Metal-Organic Frameworks for Photocatalysis *Chin. J. Chem.* **35** 135-47

[72]   Alvaro M, Carbonell E, Ferrer B, Llabrés i Xamena F X and Garcia H 2007 Semiconductor Behavior of a Metal-Organic Framework (MOF) *Chem. Eur. J.* **13** 5106-12

[73]   Gao X, Zhai M, Guan W, Liu J, Liu Z and Damirin A 2017 Controllable Synthesis of a Smart Multifunctional Nanoscale Metal-Organic Framework for Magnetic Resonance/Optical Imaging and Targeted Drug Delivery *ACS Appl. Mater. Inter.* **9** 3455-62

[74]   Qin J-S, Yuan S, Wang Q, Alsalme A and Zhou H-C 2017 Mixed-linker strategy for the construction of multifunctional metal–organic frameworks *J. Mater. Chem. A* **5** 4280-91

[75]   Pullen S and Ott S 2016 Photochemical Hydrogen Production with Metal–Organic Frameworks *Top. Catal.* **59** 1712-21

[76]   Deng X, Li Z and Garcia H 2017 Visible Light Induced Organic Transformations Using Metal-Organic-Frameworks (MOFs) *Chem. Eur. J.* 23 1-22

Captions for Figures

Fig. 1 (a). XRD patterns of the as-obtained MOF-253 (i), MOF-253-Re(CO)$_3$Cl (ii), sensitized-MOF-253-Re(CO)$_3$Cl (iii)MOF-253 and calculated MOF-253 (iv). (b). FT-IR spectra of MOF-253-Re(CO)$_3$Cl (i) and Re(CO)$_5$Cl (ii). (c). N$_2$ adsorption/desorption isotherms (77 K) of MOF-253-Re(CO)$_3$Cl (i) and Re(CO)$_5$Cl (ii). (d). UV/Vis DRS spectra of MOF-253 (Solid line), MOF-253-Re(CO)$_3$Cl(Dot line) and sensitized-MOF-253-Re(CO)$_3$Cl (Dash line), UV/Vis absorption spectrum of homogeneous Re(dcbpy)(CO)$_3$Cl (Inset figure).

Fig. 2 (a). The respective TON of H$_2$ (■), CO (●), HCOO$^-$ (▲) over MOF-253-Re(CO)$_3$Cl and the t-TON (△) over filtrated solvent. (b). The t-TON over MOF-253-Re(CO)$_3$Cl (□), and Re(dcbpy)(CO)$_3$Cl (△).

Fig. 3 XRD patterns for MOF-253-Re(CO)$_3$Cl after (i) and before (ii) the photocatalytic reaction.

Fig. 4 TON comparsion between MOF-253-Re(CO)$_3$Cl and sensitized-MOF-253-Re (CO)$_3$Cl after 4h irradiation.

Captions for Schemes

Scheme 1 General mechanism for photocatalytic CO$_2$ reduction over [Re(N, N')(CO)$_3$X].

Scheme 2 Proposed mechanism for photocatalytic CO$_2$ reduction over the as-prepared MOF-253-Re(CO)$_3$Cl under visible light.

Captions for Tables

Table 1 TON for photocatalytic CO$_2$ reduction with as-obtained samples under variety conditions.
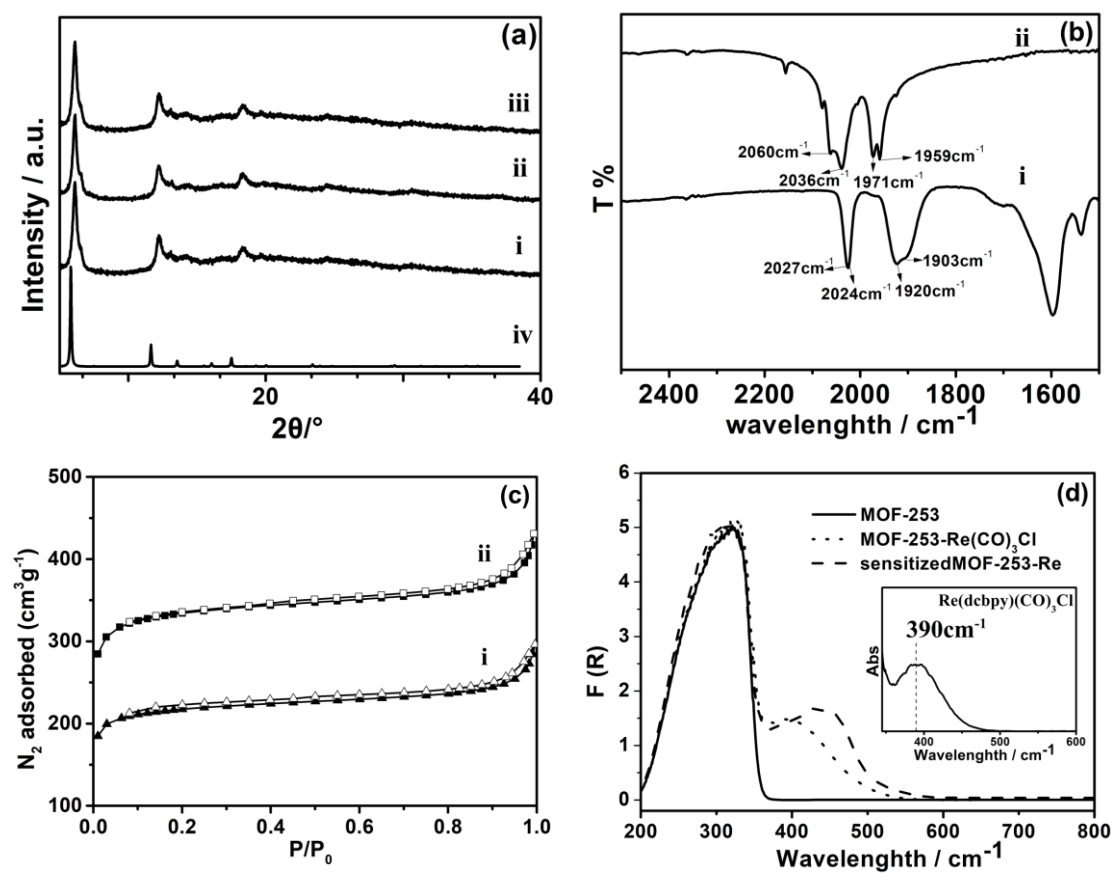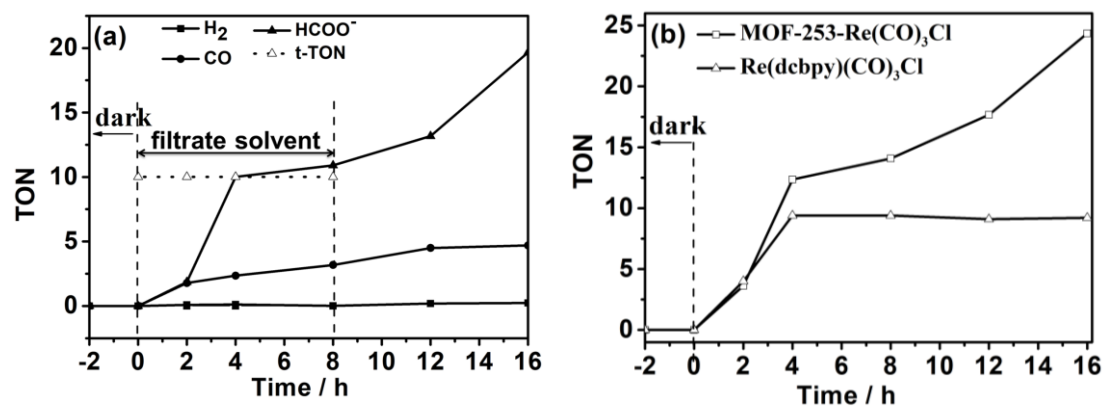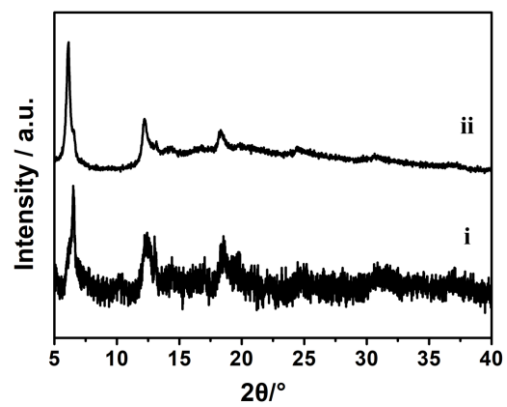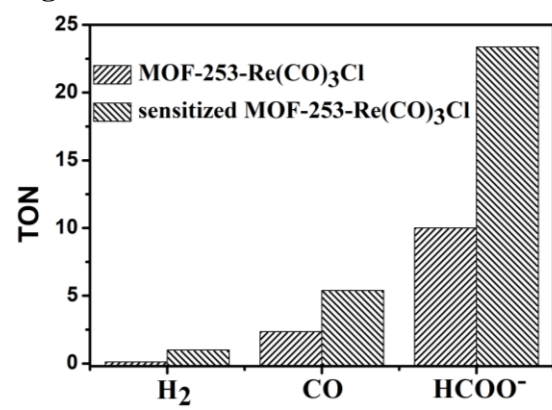
Fig. 1

(a)
Intensity / a.u.

iii
ii
i
iv

2θ/°

(b)
T %

ii

2060cm⁻¹ → ← 1959cm⁻¹
2036cm⁻¹ 1971cm⁻¹

i

2027cm⁻¹ → ← 1903cm⁻¹
2024cm⁻¹ 1920cm⁻¹

wavelenghth / cm⁻¹

(c)
N₂ adsorbed (cm³g⁻¹)

ii
i

P/P₀

(d)
F (R)

— MOF-253
······ MOF-253-Re(CO)₃Cl
- - - sensitizedMOF-253-Re

Re(dcbpy)(CO)₃Cl
390cm⁻¹
Abs
Wavelenghth / cm⁻¹

Wavelenghth / cm⁻¹

Fig. 2

Fig. 3

Fig. 4
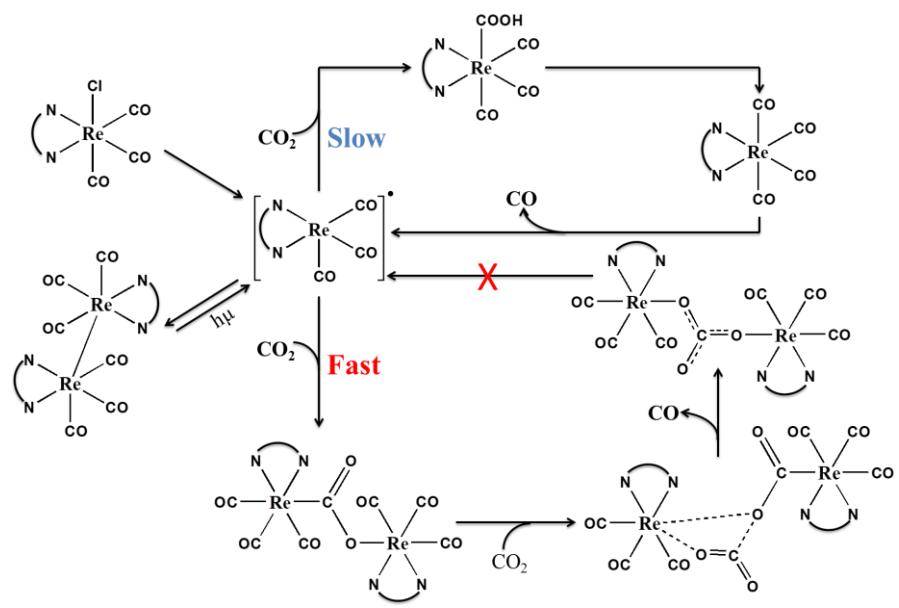
Scheme 1

Scheme 2
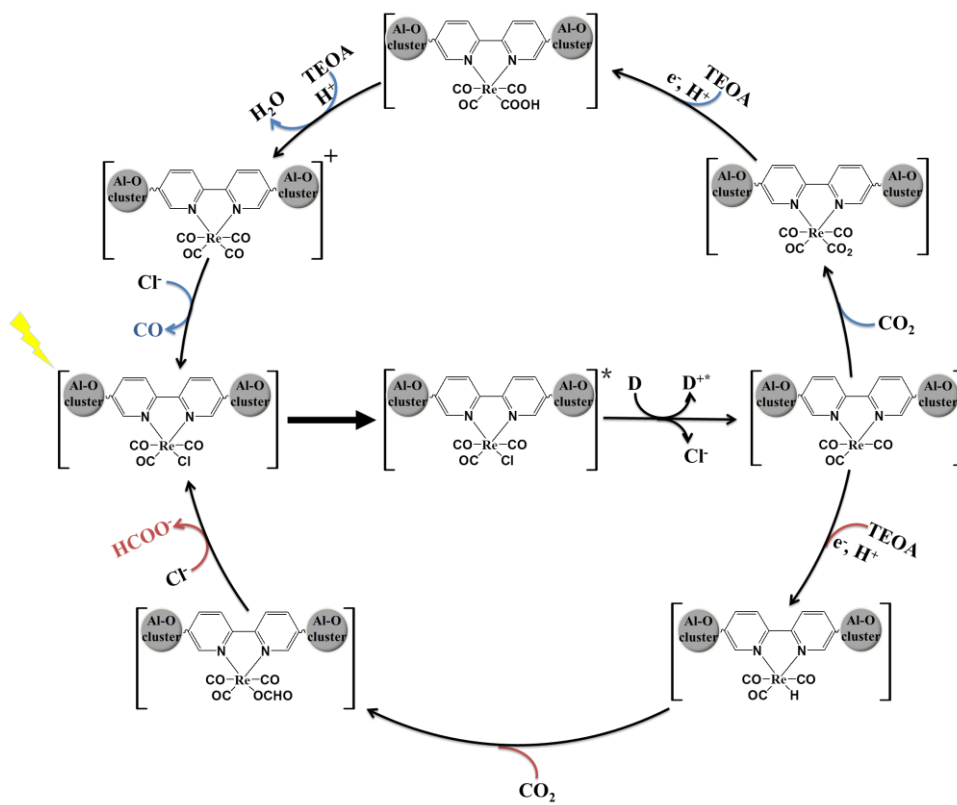
Table 1

Entry	Cat.	Solvent	Sacrificial agent	TON(Products)[a]			
				H_2	CO	$HCOO^-$	$CO+HCOO^-$
1	MOF-253-Re(CO)$_3$Cl	DMF/H$_2$O	TEOA	0.1	2.4	10.0	12.4
2	MOF-253	DMF/H$_2$O	TEOA	0.03	0.01	0	0.01
3[b]	MOF-253-Re(CO)$_3$Cl	DMF/H$_2$O	TEOA	0	0	0	0
4[c]	MOF-253-Re(CO)$_3$Cl	DMF/H$_2$O	TEOA	0.23	0	0	0
5	MOF-253-Re(CO)$_3$Cl	THF/H$_2$O	TEOA	0.1	0.6	5.2	5.8
6	MOF-253-Re(CO)$_3$Cl	DMF/H$_2$O	TEA	0.4	0.8	0.8	1.6
7	MOF-253-Re(CO)$_3$Cl	DMF/H$_2$O	-	0	0	0	0
8[d]	Re(dcbpy)(CO)$_3$Cl	DMF/H$_2$O	TEOA	0.02	9.4	0	9.4
9	Sensitized-MOF-253-Re(CO)$_3$Cl	DMF/H$_2$O	TEOA	1.0	5.4	23.4	28.8
10	MOF-253-Ru	DMF/H$_2$O	TEOA	0.02	0.08	0.6	0.68
11[e]	[Ru(bpy)$_2$Cl$_2$]$_2$	DMF/H$_2$O	TEOA	0.1	0.02	0.1	0.1

Conditions: catalyst (5 mg), solvent (DMF:H$_2$O=25:1, 3.4 mL), sacrificial agent (0.6 ml), visible light irradiation(400nm≤λ≤800 nm), under CO$_2$ atmosphere. Reaction time (4h). [a] The evolution of gaseous products and liquid products was calculated by GC and IC respective, TON is defined as mole of the evolved H$_2$ CO and HCOO$^-$ over per amount of Rhenium, [b] no light, [c] under N$_2$ atmosphere, [d] catalyst (2 mg), [e] catalyst (2 mg), TON calculated by the mole of ruthenium in catalyst.